JLB

PIVOTAL ADVANCE

# Pivotal Advance: Nonfunctional lung effectors exhibit decreased calcium mobilization associated with reduced expression of ORAI1

*Subhashini Arimilli, Sharad K. Sharma, Rama Yammani, Sean D. Reid, Griffith D. Parks, and Martha A. Alexander-Miller*[1]

Department of Microbiology and Immunology, Wake Forest University School of Medicine, Winston-Salem, North Carolina, USA

RECEIVED AUGUST 26, 2009; REVISED DECEMBER 17, 2009; ACCEPTED DECEMBER 19, 2009. DOI: 10.1189/jlb.0809575

## ABSTRACT

**CD8$^+$ T cells play a critical role in the clearance of respiratory pathogens. Thus, it is surprising that functional inactivation of lung effectors has been observed in many models of viral infection. Currently, the molecular defect responsible for the shut-off of function in these cells is unknown. In the present study, we addressed this question using a model of respiratory infection with the paramyxovirus SV5. Nonfunctional cells were found to exhibit decreases in SOCE, resulting in reduced NFAT1 activation. Notably, function could be restored by the provision of increased levels of extracellular calcium. The reduced ability to mobilize calcium was associated with reduced expression of ORAI1, the CRAC channel subunit. These findings reveal a previously unknown mechanism for the negative regulation of function in effector T cells. *J. Leukoc. Biol.* 87: 977–988; 2010.**

## Introduction

T cells that lack effector function have been reported extensively (e.g., refs. [1–9]). Classically, these cells arise as a result of inappropriate activation of naïve T cells, e.g., engagement of p/MHC in the absence of costimulatory molecules or cytokines (for review, see ref. [9]). However, there are an increasing number of studies showing loss of cytokine production and/or lytic capability in cells that were fully functional previously [1–5]. This has been reported in cases of chronic infection, e.g., LCMV clone 13, HIV, or HCV, wherein effectors encounter their cognate antigen repeatedly over a long period of time [6–8], and in TIL, where regulatory cytokines and cells present at the tumor site can inhibit T cell function [10]. Significant effort has been expended to identify the molecular defect responsible for the inability of such effector cells to function upon encounter with antigen. Perhaps not surprisingly, the responsible defect differs depending on the nature of the regulatory event. In the case of TIL, a recent report demonstrated that loss-of-function can result from dissociation of the CD8 from the TCR [11]. In addition, tumor-associated loss-of-function in effector T cells can occur through regulation by tumor-associated myeloid suppressor cells, which induce nitration of tyrosines on CD8 and TCR molecules, resulting in the inability of these molecules to bind p/MHC complexes [12]. Further, there are a number of examples of active negative regulation of the TCR signal transduction pathway. For example, cells rendered anergic by a variety of approaches have been shown to exhibit defects in the activation of the Ras/MAPK signaling pathway, which correlate with the expression of factors that can negatively regulate signaling, e.g., ubiquitin ligases, such as Itch, Grail, and cbl-b, or DKG$\alpha$, which converts DAG into PA (for review, see refs. [13–15]).

Our laboratory is focused on understanding the regulation of effector function in T cells that enter into the specialized microenvironment of the lung. Our previous studies showed that over time, an increasing percentage of virus-specific CD8$^+$ T cells, generated following respiratory infection with the paramyxovirus SV5, becomes impaired in their ability to produce cytokines or release lytic granules as a result of residence in the lung [5]. Loss-of-function in lung resident effector cells has also been reported in a number of other models, including respiratory syncytial virus [1, 2], influenza virus [2], mouse pneumovirus [3], and LCMV [4]. Recently, we found that the

Abbreviations: 2-APB=2-aminoethyldiphenyl borate, APC=allophycocyanin, CRAC=calcium release-activated calcium, Ct=critical threshold cycle, DAG=diacylglycerol, DKG$\alpha$=DAG kinase $\alpha$, ER=endoplasmic reticulum, Fluo-3=Fluo-3 acetyoxymethylester, FSC=forward-scatter, ICCS=intracellular cytokine staining, LCMV=lymphocytic choriomeningitis virus, MFI=mean fluorescence intensity, miRNA=microRNA, PA=phosphatidic acid, p.i.=postinfection, p/MHC=peptide MHC, SHP-1=Src-homology-2-domain-containing protein tyrosine phosphatase 1, SOCE=store-operated calcium entry, SSC=side-scatter, STIM1=stromal interaction molecule 1, SV5=simian virus 5, TIL=tumor-infiltrating lymphocytes

1. Correspondence Department of Microbiology & Immunology, Room 5140 Gray Building, Wake Forest University School of Medicine, Medical Center Blvd., Winston-Salem, NC 27157, USA. E-mail: marthaam@wfubmc.edu

0741-5400/10/0087-977 © Society for Leukocyte Biology

loss-of-function can also occur in the effector $CD8^+$ T cells that enter the lung in the absence of infection [16], suggesting that a signal present in the basal lung environment is capable of mediating this effect. Whether the molecular mechanism responsible for the loss-of-function is shared among these models or whether distinct mediators are at play is currently unknown. However, the consistent finding among these studies—that effectors entering into the lung become functionally impaired—suggests that the dampening of T cell responses in the lung is a general rule. Certainly, a clearer understanding of the mechanism responsible for the failure of these cells to exhibit effector function is an important goal.

In the present study, we approached this issue by determining how TCR signaling was modified in cells that had become nonfunctional following entry into the lung. TCR signaling is known to culminate in the activation of NFAT1, NF-κB, and AP-1. From previous studies, it is clear that NFAT1 activation/regulation plays a critical role in the control of effector function in $CD8^+$ T cells [17, 18] as well as in the induction of anergy [19, 20]. NFAT1 resides in the cytoplasm in an inactive form. Following TCR engagement, intracellular calcium stores are released from the ER. This results in the activation of the ER resident STIM1 molecule, which then comes into proximity with the plasma membrane to signal opening of CRAC channels [17, 21, 22]. Phase two of the signal is then initiated, as extracellular calcium is brought inside the cell at a high level. The resulting, sustained increase in calcium results in the activation of NFAT1 (for review, see ref. [17]). Once activated, NFAT1 translocates to the nucleus, where it binds to regulatory sequences and regulates the expression of many genes, including several cytokines, e.g., IFN-γ [23, 24].

In the studies presented here, we found that lung resident $CD8^+$ effector cells that had lost function exhibited reduced levels of total and activated NFAT1. Results suggested that the reduced NFAT1 activation was a result of a decrease in the ability to mobilize calcium. Consistent with this, increases in the level of extracellular calcium in conjunction with TCR engagement resulted in NFAT1 nuclear localization and restoration of function. Given the importance of CRAC channels in mediating increased intracellular calcium levels, we investigated the function and expression of the CRAC channel. Our studies revealed that the ORAI1 (the subunit that forms the channel) message and protein were reduced in nonfunctional cells, suggesting a novel mechanism, whereby limiting CRAC channel expression serves to negatively regulate function in effector T cells.

## MATERIALS AND METHODS

### Mice and recombinant viruses

Six- to 8-week-old female BALB/c mice were purchased from the Frederick Cancer Research and Development Center (Frederick, MD, USA). All research performed complied with federal and institutional guidelines set forth by the Wake Forest University Animal Care and Use Committee (Winston-Salem, NC, USA). The recombinant wild-type SV5 virus was purified by centrifugation (25,000 rpm, 6 h, SW28 rotor) through a 20% glycerol cushion, resuspended in DMEM with 0.75% BSA, and titrated on CV-1 cells as described previously [25].

### Immunizations

Mice were immunized as described previously [26]. Briefly, mice were anesthetized with Avertin (2,2,2-tribromoethanol; Sigma Chemical Co., St. Louis, MO, USA) by i.p. injection. PFU ($1\times10^6$) of virus in PBS was delivered intranasally in a volume of 50 μl.

### Staining and analysis of lung-derived $CD8^+$ T cells

Lungs were removed at the indicated day p.i. with SV5. Lung tissue was minced and incubated in the presence of 100 mg/ml collagenase D (Sigma Chemical Co.) for 45–60 min at 37°C. Digested lung tissue was then passed through a 70-μ filter and mononuclear cells enriched by density gradient centrifugation using Histopaque 1077 (Sigma Chemical Co.). Isolated cells were labeled with APC-conjugated SV5-$M_{285–293}/L^d$ tetramer (provided by the National Institutes of Health Tetramer Core Facility) and anti-CD8α-PerCp-Cy5.5 antibody (clone 53-6.7) and in some cases, anti-CD69-PE or anti-CD25-PE (all from BD Biosciences, San Jose, CA, USA) by incubation for 30 min on ice. Following washing, samples were acquired on a BD Biosciences FACSCalibur flow cytometer and data analyzed using CellQuest software (BD Immunocytometry Systems, San Jose, CA, USA) or FlowJo Software (Treestar, Inc., Ashland, OR, USA). For NFAT1 analyses, isolated cells were fixed and permeabilized followed by staining with anti-NFAT1 antibody (2 μg/ml; BD Biosciences) and anti-mouse IgG conjugated with AlexaFluor488.

### Analysis of cytokine production and ORAI1 protein

Lymphocytes isolated from the lung as described above were cultured for 5 h in 96-well, round-bottom plates (Becton Dickinson Labware, Franklin Lakes, NJ, USA) at a concentration of $1 \times 10^6$ cells/well in a volume of 200 μl complete medium [RPMI 1640 supplemented with 2 mM L-glutamine, 0.1 mM sodium pyruvate, nonessential amino acids, 100 U/mL penicillin, 100 μg/mL streptomycin, 2-ME (0.05 mM), and 10% FBS] containing monensin (GolgiPlug, BD PharMingen, San Diego, CA, USA). Where indicated, stimulation was carried out in the presence of 1 μM $M_{285–293}$ peptide or tetramer. As noted, in some cases, titrated amounts of $CaCl_2$ (50–0.39 mM) were added. Following culture, the cells were harvested, washed, and incubated with anti-CD8 antibody for 30 min on ice. After washing, cytokine production was assessed by intracellular cytokine using the Cytofix/Cytoperm kit according to the manufacturer's instructions (BD Biosciences) and staining with antibodies to IFN-γ and TNF-α (BD Biosciences) where indicated. In cases where the ORAI1 antibody was used in conjunction with IFN-γ staining, 0.4 μg ORAI1 polyclonal antibody (sc-74778, Santa Cruz Biotechnology, Inc., Santa Cruz, CA, USA) was added to fixed and permeabilized cells, followed by a FITC-labeled anti-goat secondary antibody. Normal goat IgG (sc-2028, Santa Cruz Biotechnology, Inc.) was used as an isotype control.

### Isolation of functional and nonfunctional $M_{285–293}$-specific lung cells

Isolated lung lymphocytes were stimulated for 4 h with SV5-$M_{285–293}/L^d$ tetramer in a 24-well plate ($10^7$ cells/ml). IFN-γ-producing cells were isolated by sorting using the mouse IFN-γ secretion assay kit (Miltenyi Biotec, Auburn, CA, USA), as per the manufacturer's instructions with minor modifications. Briefly, following the 4-h stimulation period, cells were collected and washed with 2 ml cold MACS buffer, followed by labeling with the supplied mouse IFN-γ catch reagent. All wash steps and the wash buffer volumes recommended by the manufacturer were reduced by half, as this was found to increase cell recovery. Prewarmed medium was added to the cells, and the cultures rotated for 40 min at 37°C. IFN-γ-secreting cells were identified by incubation with the PE-labeled IFN-γ detection antibody. Concurrently, cells were labeled with PerCp-Cy5.5-conjugated anti-CD8 antibody. For isolation of $CD25^+$ versus $CD25^-$ cells, lung cells were stimulated with SV5-$M_{285–293}/L^d$ tetramer for 4 h, followed by staining with anti-CD25 and anti-CD8 antibodies. For sorting, cells were first gated through FSC/SSC and SV5-$M_{285–293}/L^d$ tetramer/CD8 gates. Sorting was performed using a FACSAria high-speed cell sorter (BD Immunocytometry Systems).

### Measurement of intracellular calcium

Intracellular calcium flux was measured by flow cytometry using the calcium-sensitive dye Fluo-3. IFN-$\gamma^+$/IFN-$\gamma^-$ or CD25$^+$/CD25$^-$ cells sorted as above were rested overnight in complete media with 5% T-stim (to promote survival). Cells were loaded with the calcium-sensitive dye Fluo-3 (4 uM) by incubation for 30 min at 37°C. Following washing, cells were resuspended in PBS without calcium or magnesium. Basal Fluo-3 fluorescence was determined by measurement for 60 s. PMA (50 ng/ml) and ionomycin (1 $\mu$g/ml) were then added and fluorescence measured for an additional 220 s to evaluate calcium release from intracellular stores followed by addition of $CaCl_2$ (0.5 mM). Fluorescence measurements were acquired for an additional 200 s. In cases where anti-CD3 antibody was used for activation, cells were preincubated with 5 $\mu$g/ml biotinylated anti-CD3. Baseline readings were obtained for 60 s, followed by addition of 10 $\mu$g/ml streptavidin. Measurements post-streptavidin addition were taken as described above. Data analysis was performed using FlowJo software (Tree Star, Inc., Ashland, OR, USA).

### 2-APB treatment

Functional versus nonfunctional $M_{285–293}$-specific cells were sorted based on expression of CD25. Isolated populations were loaded with Fluo-3 as above. Basal Fluo-3 fluorescence was determined by measurement for 60 s, following which PMA (50 ng/ml) and ionomycin (1 $\mu$g/ml) were added and fluorescence analyzed for an additional 120 s to evaluate calcium release from intracellular stores. $CaCl_2$ (0.4 mM) was then added, and readings continued for an additional 240 s. At this point, 2-APB (3 $\mu$M; Sigma Chemical Co.) was added and fluorescence measured for an additional 200 s.

### NFAT1 localization

Following resting overnight, IFN-$\gamma^+$/IFN-$\gamma^-$ or CD25$^+$/CD25$^-$ cells were stimulated for 15 min with immobilized anti-CD3 (previously coated poly-L-lysine coverslips in 24-well plate coated with 1 $\mu$g/ml antibody in PBS) at 37°C, followed by fixation with warm 3% ultrapure paraformaldehyde (Polysciences Inc., Warrington, PA, USA; 10 min at 37°C) and permeabilization with Cytofix/Cytoperm. Cells were washed and stained at 25°C for 30 min with NFAT1 (2 $\mu$g/ml; Affinity BioReagents, Golden, CO, USA), followed by anti-mouse Rhodamine Red for 30 min. DAPI Gold (Molecular Probes, Carlsbad, CA, USA) was used to mount the cells. Images were acquired using a Zeiss LSM 510 confocal microscope and analyzed using LSM Image software.

### Western blot analysis

IFN-$\gamma^+$ or IFN-$\gamma^-$ cells, obtained by sorting as above, were rested overnight, followed by stimulation with immobilized anti-CD3 antibody and anti-CD28 antibody (30 min at 37°C). Cells were then washed with cold PBS and lysed with buffer containing 1% Triton X-100, 20 mM Tris (pH 7.4), 150 mM NaCl, 1 mM EDTA, 2.5 mM sodium pyrophosphate, 10 mM NaF, 1 mM $Na_2VO_4$, and 1 ug/ml leupeptin. Cell lysates were solubilized in reducing Laemmli sample buffer, and $10^5$ cell equivalents were loaded and resolved by 12% SDS-PAGE. Gels were transferred onto nitrocellulose membranes (Millipore Inc., Billerica, MA, USA), which were blocked with 3% BSA for 1 h, followed by addition of anti-NFAT1 antibody (10 $\mu$g/ml; BD Biosciences). HRP-conjugated goat anti-mouse antibody (0.2 $\mu$g/ml; Jackson ImmunoResearch Laboratories, Inc. West Grove, PA, USA) was added, followed by detection with SuperSignal chemiluminescent substrate (Millipore Inc.). Band density was determined using Image J software. NFAT1 band readings were normalized to the actin control.

### ORAI1 and STIM1 mRNA measurement

After sorting, CD25$^+$ and CD25$^-$ cells were washed once with PBS and lysed in 200 $\mu$l Trizol. TaqMan gene expression assays (Applied Biosystems, Foster City, CA, USA) were used to measure the transcript levels of *orai1* and *stim1* by real-time RT-PCR. TaqMan assays were performed with an ABI 7000 instrument (Applied Biosystems) as described previously [27]. Briefly, RT-PCR was performed with the TaqMan One-Step RT-PCR Master Mix reagents kit (Applied Biosystems) as described by the manufacturer. The amplification profile used was as follows: one cycle at 48°C for 30 min, one cycle at 95°C for 10 min, and 50 cycles at 95°C for 15 s and 60°C for 1 min. The Ct is defined as the cycle at which fluorescence becomes detectable above background levels and is inversely proportional to the logarithm of the initial concentration of template. A standard curve was plotted for each reaction with Ct values obtained from amplification of known quantities of murine genomic DNA. The standard curves were used to transform Ct values of the experimental samples to the relative number of DNA molecules. The quantity of cDNA for each experimental gene was normalized to the quantity of the constitutively transcribed control gene (18 s rRNA) in each sample. This control was chosen based on a previous report demonstrating that 18 s rRNA expression levels are highly stable in T lymphocytes, and therefore, this message is optimal for normalization [28]. Samples were assayed in duplicate and specific transcript levels expressed as fold difference between the conditions compared.

## RESULTS

### Nonfunctional cells retain the ability to express CD69 but not CD25 in response to TCR engagement

We have reported previously that a large percentage of CD8$^+$ effector cells that enter the lung following respiratory infection with SV5 become nonfunctional; i.e., they cannot produce cytokines or lyse target cells [5]. At time-points that coincide with initial entry of effectors into the lung (i.e., Day 7 p.i.), nearly all of the immunodominant $M_{285–293}$-specific effector cells are functional [5]. However, by Day 12 p.i., ~50% of the $M_{285–293}$-specific cells are no longer capable of producing cytokine or lysing infected cells. This dysregulation continues for an extended period of time, and nearly 85% of the cells are identified as nonfunctional by Day 40 p.i. [5].

We knew that the $M_{285–293}$-specific effectors that are unable to produce cytokine or release lytic granules could still internalize TCR and undergo limited proliferation in response to TCR engagement (our unpublished data and ref. [16]). These findings suggested that TCR engagement resulted in at least partial signaling in nonfunctional cells. To gain additional insights into the ability of these cells to respond to TCR engagement, we determined whether nonfunctional cells retained the ability to express CD25 or CD69. Lung lymphocytes were isolated from BALB/c mice on Day 12 p.i. with SV5. For these experiments, we used the APC-labeled SV5-$M_{285–293}$/$L^d$ tetramer in combination with peptide antigen as the stimulus for IFN-$\gamma$ production. This approach serves to identify all SV5-$M_{285–293}$-specific cells simultaneously, as well as to trigger function. Preliminary studies were carried out to ensure that the conditions used were capable of inducing IFN-$\gamma$ production in all functional cells (data not shown). Interestingly, we found that SV5-specific effector cells were capable of expressing CD69, regardless of their ability to produce cytokine (**Fig. 1**). Of note, the nonfunctional cells showed a statistically significant reduction in the percentage of cells that were CD69$^+$ (78.5% vs. 89.0%, Fig. 1B). However, the large majority of nonfunctional cells does express this molecule. The ability to express CD69 provides additional support for the model that cells that are incapable of producing cytokines or effecting lysis have some ability to respond. In contrast, CD25 expression correlated with the ability to produce IFN-$\gamma$ (Fig. 1). On

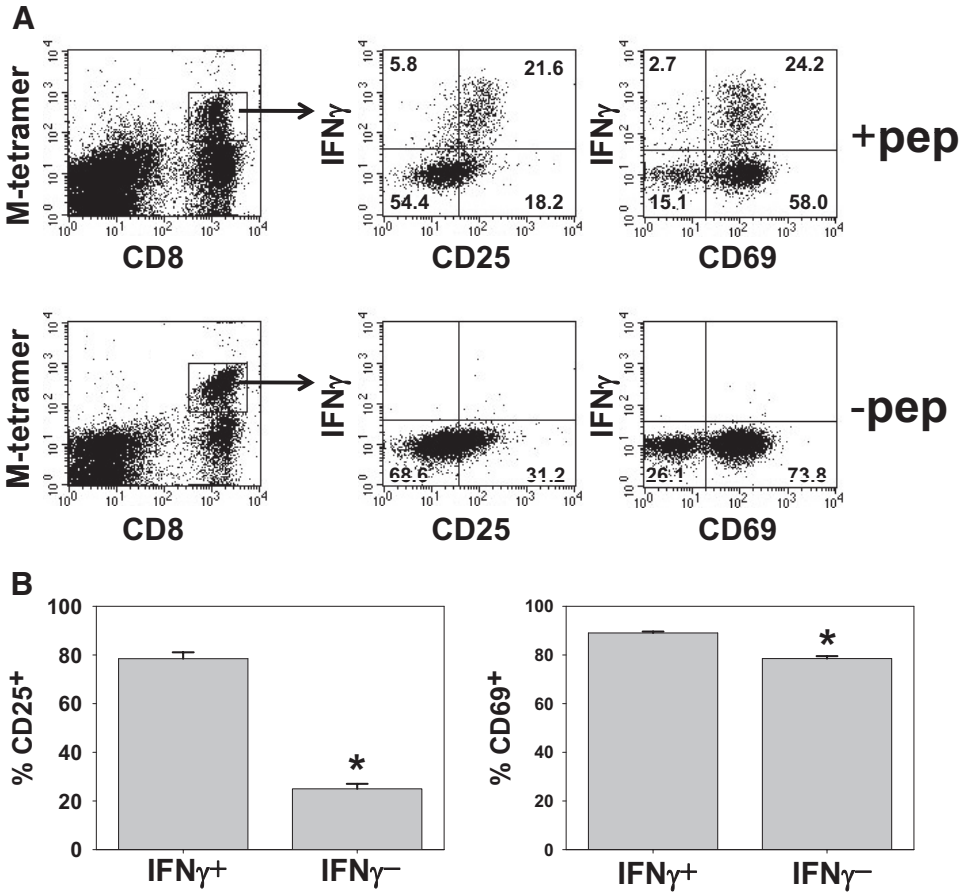


**Figure 1. Nonfunctional cells retain the ability to up-regulate CD69 but not CD25 in response to TCR engagement.** Mice were intranasally infected with SV5, and on Day 12, p.i. lung cells were isolated and stimulated with SV5-$M_{285–293}/L^d$ tetramer for 4 h. Cells were then stained for CD8, IFN-γ, and CD69 or CD25 expression. Tetramer$^+$CD8$^+$ cells were gated, and IFN-γ production versus CD25 and CD69 expression was analyzed. Representative data are shown in A. The expression of CD69 or CD25 following culture in the presence (+pep; upper panels) or absence (–pep; lower panels) of peptide stimulation is shown versus IFN-γ production. These data are representative of three independent experiments, each containing three individually analyzed animals. (B) Averaged data for the nine animals analyzed in the three independent experiments are shown. *, $P < .001$.

average, 78.5% of functional cells expressed CD25 in comparison with 25.0% of nonfunctional cells (Fig. 1B). Analysis of the expression of CD69 and CD25 in cells that were cultured in the absence of peptide showed that a large percentage of cells capable of expressing CD25 and CD69 already expressed these markers in the absence of restimulation with peptide in vitro (Fig. 1A, lower panels). However, restimulation with peptide was required to detect all cells with the capacity to express these molecules. Thus, the regulation of these two activation-induced molecules is differentially affected under conditions where loss-of-function is present.

## Total and activated NFAT1 levels are reduced in nonfunctional cells

The ability to up-regulate CD69 together with the deficiencies in CD25 expression and cytokine production in $M_{285–293}$-specific cells suggested that the signal generated as a result of TCR engagement was impaired as opposed to absent. Our previous finding that PMA and ionomycin failed to rescue function pointed to a TCR distal defect [5]. As noted above, one critical result of TCR signaling is the activation of NFAT1. Thus, we hypothesized that deficiencies in the expression or activation of this key modulator could result in the impaired function observed. To test this, we first determined whether there were differences in the total level of NFAT1 protein in functional versus nonfunctional cells. Lung cells were isolated from mice on Day 12 following intranasal infection with SV5 and stimulated with $M_{285–293}/L^d$ tetramer. Functional versus nonfunctional cells were identified on the basis of CD25 expression. Flow cytometric analysis revealed that functional cells expressed twofold more total NFAT1 than nonfunctional cells (**Fig. 2**). Similar results were obtained when populations were isolated based on IFN-γ production (data not shown). Thus, loss-of-function was associated with a reduction in total NFAT1.

In resting cells, NFAT1 resides in the cytoplasm in an inactive state as a consequence of phosphorylation. Increases in cytoplasmic calcium levels following extracellular uptake lead to dephosphorylation of NFAT1, which then traffics to the nucleus, where it promotes transcription. To determine whether decreased levels of NFAT1 were associated with reduced levels of activated NFAT1, we used Western blot analysis to measure the levels of phosphorylated versus dephosphorylated NFAT1 in isolated functional and nonfunctional populations. Lung cells from infected mice were stimulated with $M_{285–293}/L^d$ tetramer as above. IFN-$\gamma^+$ versus IFN-$\gamma^-$ populations were then isolated using the cytokine capture assay that allows labeling of IFN-γ-secreting cells in the absence of fixation. The purity of the sorted IFN-$\gamma^+$ and IFN-$\gamma^-$ CD8$^+$ T cell populations was ~99% (**Fig. 3A**).

For analysis of NFAT1 activation, isolated cells were sorted and rested overnight to allow optimal responsiveness to restimulation. Following this rest period, cells were stimulated

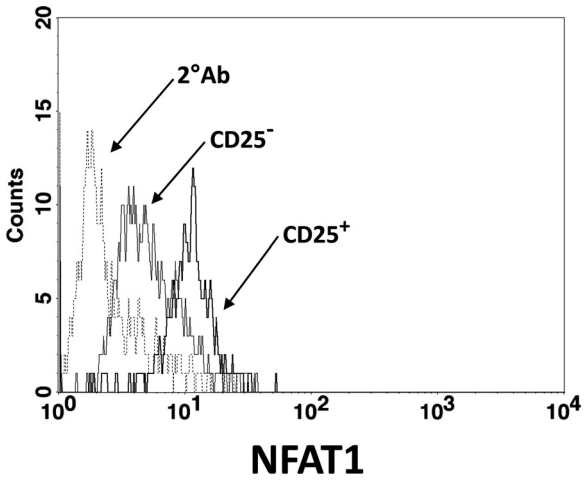


**Figure 2. Total NFAT1 is decreased in nonfunctional versus functional cells.** Lung cells from mice Day 12 p.i. with SV5 were stimulated in vitro with tetramer for 4 h. At the end of the stimulation period, cells were stained for CD25 expression and sorted in tetramer$^+$CD25$^+$ versus tetramer$^+$CD25$^-$ populations. Isolated cells were stained with anti-NFAT1 antibody. Fluorescence was measured by flow cytometry. These data are representative of three independent experiments.

with immobilized anti-CD3 and anti-CD28 antibody for 30 min. Cells were then lysed and $10^5$ cell equivalents resolved by SDS-PAGE, blotted onto nitrocellulose membrane, and probed with anti-NFAT1 antibody. Bands were quantified by densitometry with normalization to the actin control. Phosphorylated NFAT1 levels were found to be twofold higher in functional cells. Analysis of dephosphorylated NFAT1 showed that functional cells contained approximately fourfold more activated NFAT1 compared with nonfunctional cells (Fig. 3B). This difference could not be attributed solely to the twofold decrease in expression of NFAT1 in nonfunctional cells, suggesting that there was also a reduction in the extent of NFAT1 activation. As an additional measure of NFAT1 activation, we determined NFAT1 localization in the two populations. Following activation, functional versus nonfunctional cells (sorted based on CD25 expression) were fixed and stained with anti-NFAT1 antibody (Fig. 3D and E). Nonfunctional cells had limited evidence of nuclear NFAT1 staining. This is in contrast to what was observed for functional cells. Together, these data show that in addition to expressing lower levels of total NFAT1, the efficiency of activation of NFAT1 was reduced in nonfunctional cells following activation.

## Nonfunctional cells are reduced in their ability to flux $Ca^{2+}$

We next determined whether the defects in NFAT1 activation were the result of the inability of the nonfunctional cells to take up calcium from the extracellular environment in response to TCR engagement. For these experiments, lung cells were isolated from mice 12 days p.i. with SV5 and sorted into IFN-$\gamma^+$ and IFN-$\gamma^-$ populations as described above. Following overnight rest, cells were loaded with the calcium-sensitive dye Fluo-3, followed by coating with biotinylated anti-CD3 antibody. Basal Fluo-3 fluorescence levels measured for 60 s, after which, streptavidin was added to promote TCR cross-linking, and measurement continued for 220 s; 0.5 mM $CaCl_2$ was then added to monitor calcium uptake from the extracellular environment. Nonfunctional cells exhibited reduced, albeit detectable, increases in cytoplasmic calcium as a result of release from intracellular stores and subsequently, following uptake from the extracellular environment (**Fig. 4**, top panel).

Given our previous finding that function is not restored by stimulation with PMA and ionomycin [5], we predicted that activation with this stimulus would also result in reduced levels of intracellular calcium in nonfunctional cells. As expected, PMA and ionomycin stimulation of nonfunctional cells resulted in decreased calcium release from intracellular stores as well as uptake from the extracellular environment compared with functional cells (Fig. 4, middle panel). Similar results were obtained when calcium measurements were obtained from CD25$^-$ versus CD25$^+$ cells (Fig. 4, bottom panel). Together, these data suggest that there is a defect in the pathway that leads to calcium signaling.

## Addition of exogenous calcium restores function in $M_{285–293}$-specific lung effector cells

The previous data demonstrated that although reduced, nonfunctional cells did exhibit some ability to initiate calcium uptake. This suggested that CRAC channels were functioning in some capacity. Given this, we hypothesized that provision of high levels of extracellular calcium might drive increased uptake and thus, restore function in these cells. To test this hypothesis, lung effector cells were again isolated on Day 12 p.i. with SV5. Recovered cells were stimulated with $M_{285–293}$ peptide in the presence of titrated concentrations of $CaCl_2$ and IFN-$\gamma$ production assessed by ICCS. In the absence of added $CaCl_2$, cells were 58% functional (calculated by dividing the percent of CD8$^+$ cells that produce IFN-$\gamma$ by the percent that is tetramer$^+$; **Fig. 5A**). This is in agreement with levels observed in our studies published previously [5]. However, as the concentration of $CaCl_2$ increased, there was a concomitant increase in function, culminating in 94% of the $M_{285–293}$-specific cells producing IFN-$\gamma$ (Fig. 5A). This was not solely the result of the addition of $CaCl_2$, as no increase in IFN-$\gamma$ production was observed in the absence of peptide. Averaged data from three independent experiments are shown in Figure 5B. Of note, the increase in function in the presence of calcium was accompanied by a concurrent increase in CD25 expression (data not shown). Together, these data suggest that a limiting calcium signal is responsible for the failure of the effector cells to produce cytokine.

Restoration of function in the presence of $CaCl_2$ implied that the defect in NFAT1 activation was overcome in these cells. To determine if this were the case, we measured the percentage of Day 12 $M_{285–293}$-specific lung cells that exhibited nuclear localization of NFAT1 following stimulation with M-tetramer in the presence of $CaCl_2$. The results shown in Figure 5C demonstrate that in the absence of added $CaCl_2$, 50% ($\pm$1.3%) of the $M_{285–293}$-specific cells exhibited nuclear localization of NFAT1. This would be the expected distribution, given the functional capacity of this population. However, in

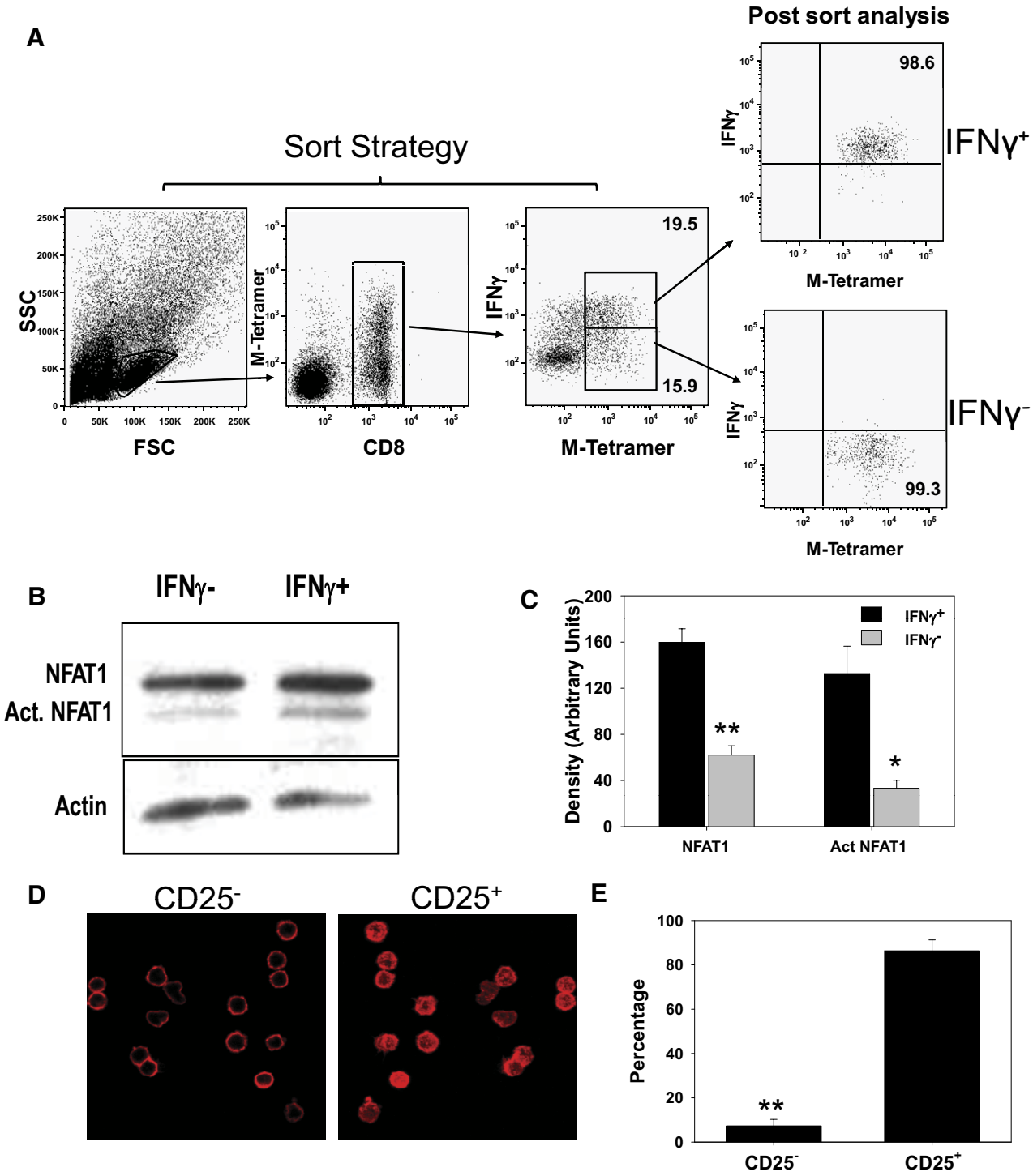


**Figure 3. NFAT1 activation and nuclear localization are decreased in nonfunctional cells.** (A) Isolated lung cells obtained from animals on Day 12 p.i. with SV5 were stimulated with tetramer for 4 h. IFN-$\gamma^+$ versus IFN-$\gamma^-$ tetramer$^+$ cells were identified using the Miltenyi cytokine capture assay and isolated using a FACSAria cell sorter. Sorted populations were highly pure. These data are representative of five independent experiments. (B and C) Isolated populations were rested overnight and then restimulated with anti-CD3 and anti-CD28 antibody for 30 min. The presence of phosphorylated versus dephosphorylated NFAT1 was then determined by immunoblot and quantified by densitometry. A representative experiment as well as averaged data from four experiments are shown. Of note, this experiment has been performed in the absence of anti-CD28 with similar results. *, $P < 0.02$; **, $P < 0.01$. (D) NFAT1 nuclear localization in isolated functional versus nonfunctional cells was analyzed by immunofluorescence. Functional versus nonfunctional cell populations were activated by culture on immobilized anti-CD3 antibody for 15 min, after which, cells were fixed and stained with the anti-NFAT1 antibody. Images were acquired using a Zeiss LSM 510 confocal microscope and are representative of five experiments. A minimum of 50 cells was analyzed in each experiment. (E) Averaged data from four independent experiments. **, $P < 0.001$.

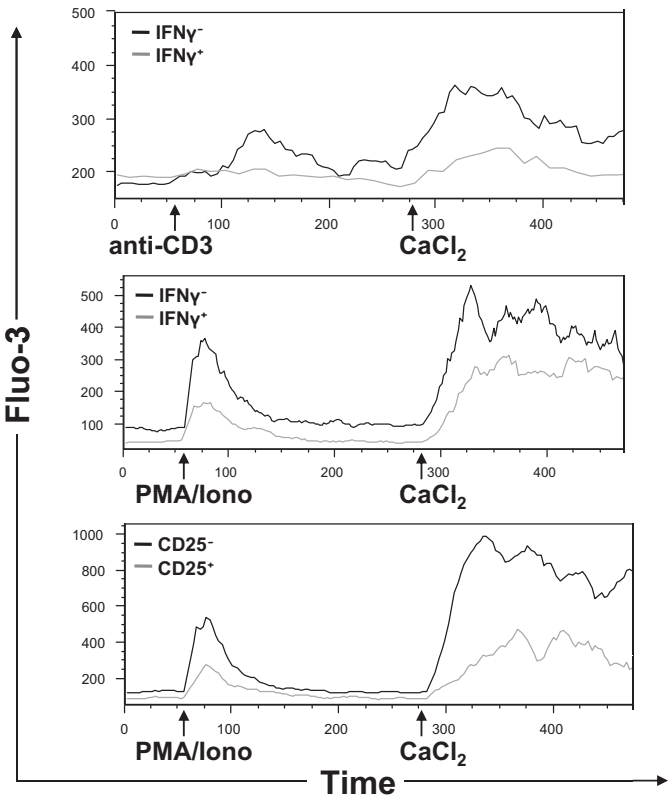


**Figure 4. Nonfunctional cells exhibit a defect in SOCE.** Lung cells isolated from mice on Day 12 p.i. with SV5 were stimulated with tetramer and IFN-$\gamma^+$ versus IFN-$\gamma^-$ or CD25$^+$ versus CD25$^-$ cells isolated by sorting. Sorted populations were incubated with Fluo-3 for 30 min at 37°C. For analysis of intracellular calcium responses following TCR engagement, cells were incubated with 5 ug/ml biotinylated anti-CD3 antibody for 15 min, after which, baseline $Ca^{2+}$ levels were assessed for 1 min. Streptavidin (10 $\mu$g/ml) was then added, and the sample was returned for measurement (top panel). For TCR-independent stimulation, baseline measurements were taken for 1 min, followed by addition of PMA (50 ng/ml) and ionomycin (Iono; 1 $\mu$g/ml; middle and bottom panels). For all conditions, 280 s after stimulation, 0.5 mM $CaCl_2$ was added to measure uptake from the extracellular environment. These data are representative of five experiments.

agreement with the data in Figure 5, A and B, in the presence of 30 mM $CaCl_2$, the percentage of cells with nuclear localization of NFAT1 was increased to 72% (±0.5%; Fig. 5C).

### CRAC channels present on IFN-$\gamma^-$ cells are functional

As the uptake of extracellular calcium in T lymphocytes depends on opening of CRAC channels [29–31], one possibility to explain the reduced calcium flux in IFN-$\gamma^-$ cells was suboptimal functioning of the channels. Alternatively, it was possible that CRAC channels were functioning efficiently but were simply reduced in number. To discriminate between these two possibilities, we tested the effect of 2-APB on calcium uptake. Addition of 2-APB at low levels (i.e., ≤10 $\mu$M) has been shown to potentiate CRAC channel-mediated uptake of extracellular calcium [32]. Isolated functional versus nonfunctional populations were stimulated with PMA and ionomycin followed by addition of $CaCl_2$ to monitor extracellular calcium uptake. In these studies, the amount of $CaCl_2$ added to evaluate uptake was reduced to allow assessment of 2-APB-induced increases. In the functional (upper panel) and nonfunctional (lower panel) populations, addition of 2-APB resulted in a robust increase in the uptake of extracellular calcium (**Fig. 6**). These findings suggested that CRAC channels in the nonfunctional cells were operating appropriately.

### Nonfunctional cells are reduced in the expression of ORAI1

Based on these results, we tested the alternative hypothesis that nonfunctional cells had reduced numbers of CRAC channels. In addition, we assessed the expression of STIM1, the regulator of CRAC channel function. Opening of the CRAC channels is dependent on dimerization of ORAI1 dimers present in the membrane [33]. Thus, reduced expression of STIM1 or ORAI1 could result in reduced entry of extracellular calcium. To test this possibility, mRNA was isolated from functional versus nonfunctional $M_{285–293}$-specific CD8$^+$ lung populations and the level of ORAI1 and STIM1 quantified by real-time RT-PCR. These studies revealed an ~7.5-fold increase in the level of ORAI1 message in functional versus nonfunctional populations, and a much more modest difference was observed in the STIM1 message (twfold higher in functional populations; **Fig. 7A**).

To determine whether there were differences in the amount of ORAI1 protein, lung cells from mice infected 12 days prior were stimulated in the presence of SV5-$M_{285–293}/L^d$ tetramer to allow concurrent labeling and activation. At the end of the 5-h stimulation period, CD8$^+$/$M_{285–293}$ tetramer$^+$ cells were assessed for ORAI1 protein and IFN-$\gamma$ by flow cytometric analysis. IFN-$\gamma^+$ versus IFN-$\gamma^-$ cells were found to differ in ORAI1. On average, functional cells expressed 1.9 ± 0.09-fold more protein compared with nonfunctional cells (Fig. 7B), suggesting reduced ORAI protein levels were correlated with loss-of-function. Interestingly, we noted that in functional cells, the level of IFN-$\gamma$ produced was correlated with the level of ORAI expression (Fig. 7C). As the MFI value for ORAI1 increased, so did the amount of IFN-$\gamma$ produced. These findings suggest that the level of ORAI1 is an important determinant of cytokine production and that the lack of function associated with reduced cytoplasmic calcium is the result of reduced expression of CRAC channels.

## DISCUSSION

Regulation of function in effector T cells is a critical factor in determining in vivo efficacy. In fact, recent publications suggest that the ability to secrete multiple cytokines as well as lyse cells, termed polyfunctionality, is a property of highly efficacious effectors [34–36]. In spite of this, it is clear that functional turn-off of effector cells does occur in vivo. Functional inactivation has been identified in antiviral T cells present during chronic infection [6–8], in tumor-infiltrating T cells (e.g., refs. [11, 12, 37]), and most recently, in cells that enter into the lung following viral infection [1–5]. In these cases, T cells initially received the signals

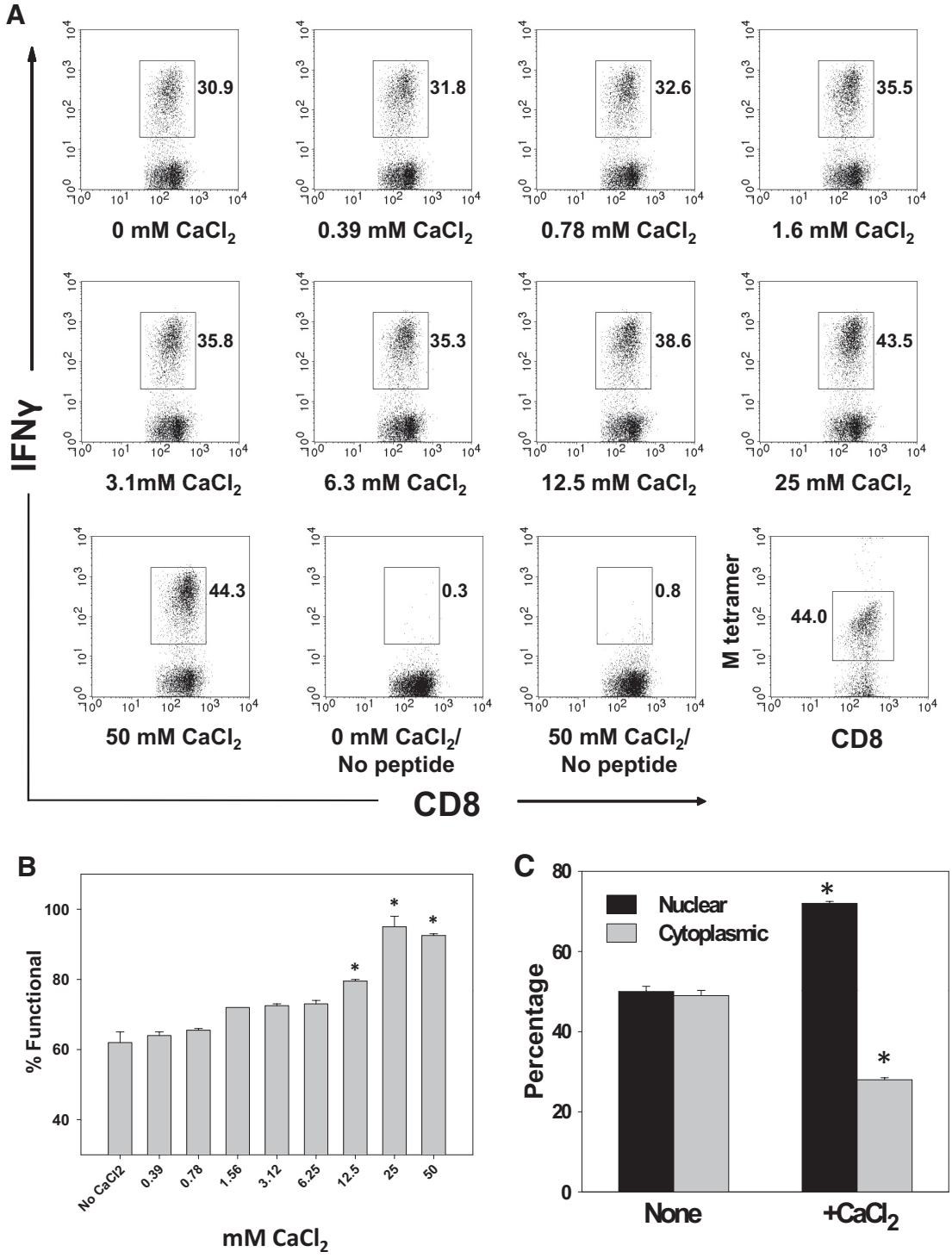


**Figure 5. Addition of $CaCl_2$ restores function in lung effector cells.** (A) Lung cells were isolated on Day 12 p.i. with SV5 and stimulated with 1 $\mu$M $M_{285–293}$ peptide in the presence of titrated concentrations of $CaCl_2$. IFN-$\gamma$ production was assessed by ICCS. In parallel, lung cells were stained with anti-CD8 antibody and tetramer. The top numbers in each graph represent the percentages of $CD8^+$ T cells that were IFN-$\gamma^+$ or tetramer$^+$, (*Continued on next page*) as indicated. (B) Averaged data from three independent experiments (mean ±SD). *, $P \leq 0.02$, compared with the absence of added $CaCl_2$. (C) Lung cells, isolated from animals on Day 12 p.i. with SV5, were cultured for 4 h in the presence of $M_{285–293}/L^d$ tetramer$^+$ ± $CaCl_2$ (30 mM). Following staining with anti-CD8 antibody, $CD8^+$/tetramer$^+$ cells were sorted, fixed, and stained with anti-NFAT1 antibody, and localization was determined by fluorescence microscopy. Seventy-five to 100 cells were counted for each condition. Averaged data from duplicate samples in two independent experiments are shown (mean±SD). *, $P \leq 0.001$, compared with untreated.

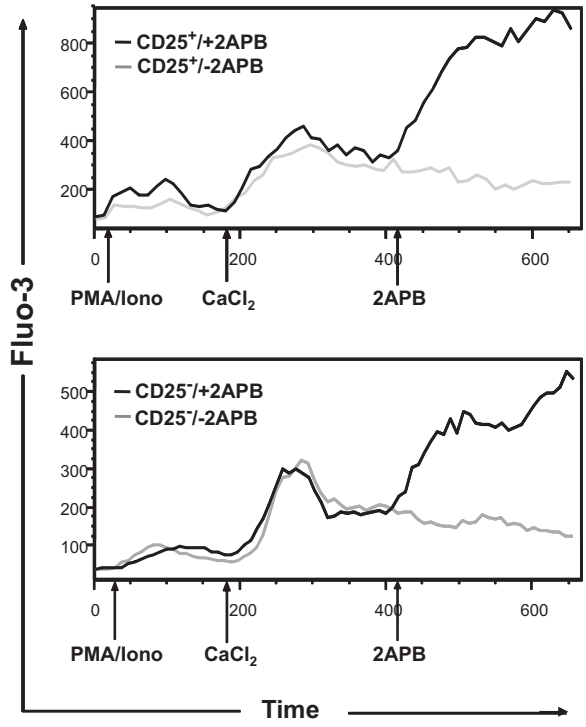


**Figure 6. Addition of 2-APB results in an increase in cytoplasmic calcium consistent with proper functioning of CRAC channels.** Lung cells isolated from mice on Day 12 p.i. with SV5 were stimulated with tetramer and tetramer$^+$CD25$^+$ versus tetramer$^+$CD25$^-$ cells isolated by sorting. Intracellular calcium responses in CD25$^+$ (upper panel) or CD25$^-$ (lower panel), following stimulation with PMA/ionomycin, were measured for 120 s. $CaCl_2$ was then added, and readings continued for 240 s. At this point, 2-APB (3 $\mu$M) was added, and fluorescence was measured for an additional 200 s. Addition of 2-APB resulted in increased uptake of calcium in functional and nonfunctional populations. These data are representative of three independent experiments.

required for appropriate activation and differentiation but in the periphery, are exposed to stimuli that over-ride this activation program, resulting in impaired function.

Significant effort has been expended to understand the molecular basis for the failure of anergized/tolerant cells to exert effector function. Calcium signaling has been shown to play a critical role in the induction of anergy, and the failure to elicit an appropriate calcium signal is a property of the anergic state [38, 39]. The current model proposes induction of anergy as a result of calcium-mediated activation of NFAT1 in the absence of/decrease in the activation of AP-1 and NF-$\kappa$B [19]. This pattern of signaling results in a program of negative regulatory gene expression. Important mediators induced include E3 ligases (e.g., Itch, Grail, and cbl-b) or DKG$\alpha$, which converts DAG into PA (for review, see refs. [13–15]). These regulators appear to work by attenuating TCR proximal signaling events. For example, Itch targets phospholipase C$\gamma$1 for ubiquitinylation [39], and cbl-b targets ZAP-70 [40]. Attenuation of these early TCR signaling events disrupts calcium signaling (as well as other events) in anergic cells. TCR proximal attenuation of signaling is also observed in nonfunctional cells present as a result of chronic infection. In the case of LCMV clone 13 and HCV infection, nonfunctional cells have been reported to express programmed death 1 [41, 42], which is thought to act through SHP-1 [43, 44], a phosphatase that is responsible for controlling the activation of Lck (for review, see ref. [45]). SHP-1 has also been proposed to be involved in abrogation of early signaling events in TIL [37].

Here, we have investigated the molecular basis for the functional dysregulation that we have reported previously in lung effector cells following paramyxovirus (SV5) infection [5]. SV5 is known to elicit a highly functional CD8$^+$ T cell response, i.e., in the draining mediastinal lymph node ($\geq$90% of CD8$^+$ effector cells that recognize the immunodominant $M_{285–293}$ peptide produce IFN-$\gamma$) [5]. Although the initial population of effectors in the lung mirrors the highly functional effector population generated in the mediastinal lymph node, over time, effectors in the lung become increasingly nonfunctional [5]. Our investigation of the downstream events associated with NFAT1 activation was directed by previous studies demonstrating a disruption of calcium signaling in anergic/tolerant cells [9, 46, 47], as well as the failure to restore function by stimulation with PMA and ionomycin, a finding that suggested a TCR distal defect [5].

The activation of NFAT1 plays a critical role in T cell activation and function. In our analyses, we found a decrease in the level of phosphorylated NFAT1 as well as a decrease in activated NFAT1. The magnitude of the decrease in the latter was greater than the former, suggesting that the reduction in activated NFAT1 could not be explained solely by a reduction in total NFAT1 protein. At present, the mechanism responsible for the decrease in total NFAT1 protein in nonfunctional cells is unclear. TCR signaling has been shown to result in an increase in NFAT1 levels [48]. One possibility is that changes in nonfunctional cells alter the TCR signal in such a way as to limit NFAT1 protein in these cells. A number of mechanisms have been reported to contribute to the control of NFAT1 protein levels, including regulated transcription, degradation by active caspase 3, miRNA-dependent control of translation, and ubiquitin-targeted protein degradation [48–51]. It is possible that alterations induced during the programming of nonresponsiveness result in an increase in the amount of miRNA184 present in cells, thereby decreasing translation of the NFAT message or increasing ubiquitinylation of NFAT1. Discriminating among these possibilities will require further study.

Within minutes of TCR stimulation, calcium is released from intracellular stores present in the ER. Loss of ER calcium stores results in the activation of STIM1, present in the ER membrane [21, 29, 30, 52–54]. It is thought that the ER plasma membrane containing activated STIM1 comes into proximity with the cellular membrane, where STIM1 induces dimerization of ORAI1 dimers, which are the subunits of CRAC channels [33]. This tetramerization allows CRAC channels to open and promote influx of calcium from the extracellular environment, activating calmodulin, which in turn, activates the phosphatase calcineurin. Dephosphorylation of NFAT1 by calcineurin results in its translocation to the nucleus, where it promotes transcription of numerous genes, including IFN-$\gamma$ [23, 24].

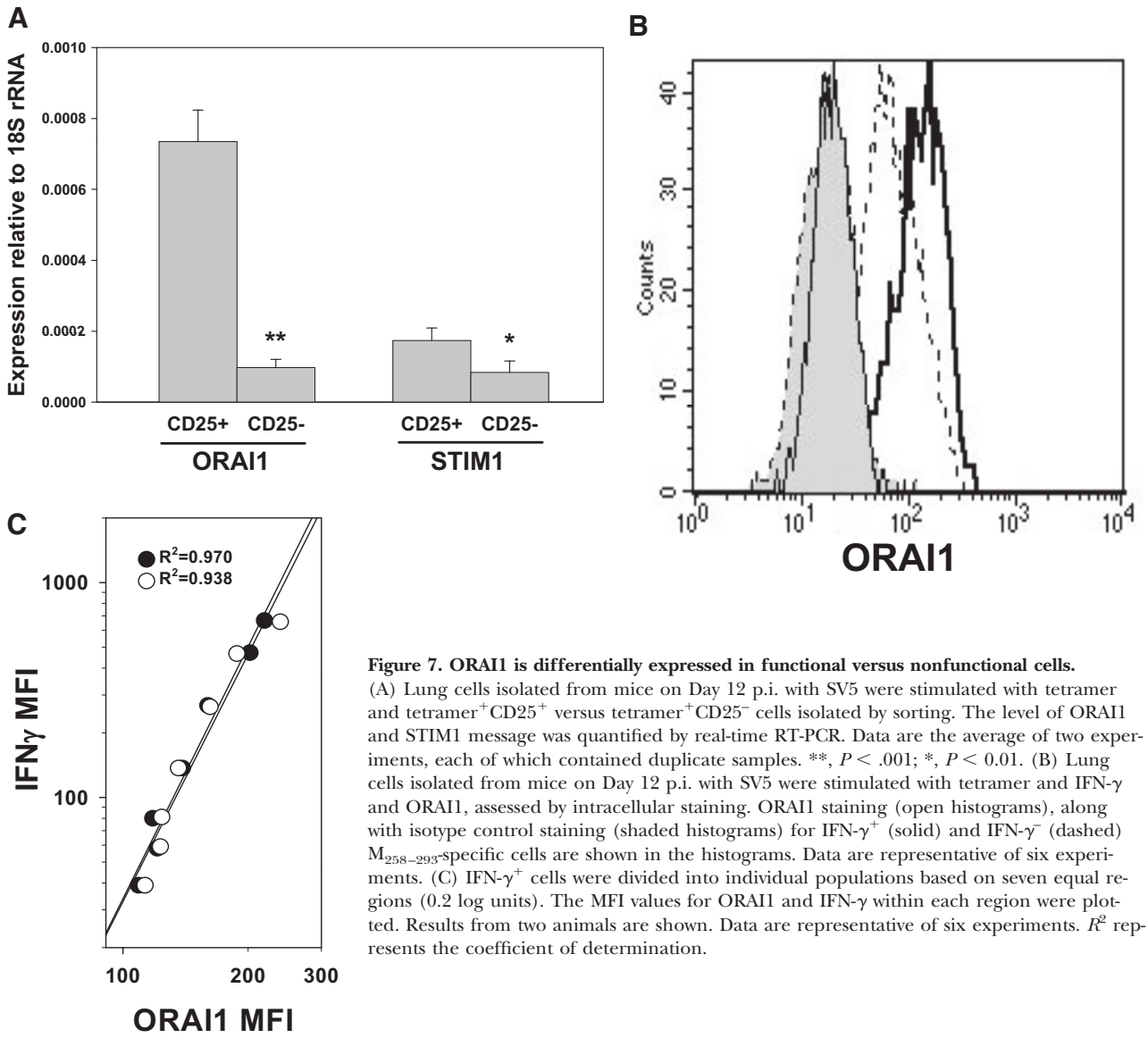


**Figure 7. ORAI1 is differentially expressed in functional versus nonfunctional cells.** (A) Lung cells isolated from mice on Day 12 p.i. with SV5 were stimulated with tetramer and tetramer$^+$CD25$^+$ versus tetramer$^+$CD25$^-$ cells isolated by sorting. The level of ORAI1 and STIM1 message was quantified by real-time RT-PCR. Data are the average of two experiments, each of which contained duplicate samples. **, $P < .001$; *, $P < 0.01$. (B) Lung cells isolated from mice on Day 12 p.i. with SV5 were stimulated with tetramer and IFN-γ and ORAI1, assessed by intracellular staining. ORAI1 staining (open histograms), along with isotype control staining (shaded histograms) for IFN-$\gamma^+$ (solid) and IFN-$\gamma^-$ (dashed) $M_{258-293}$-specific cells are shown in the histograms. Data are representative of six experiments. (C) IFN-$\gamma^+$ cells were divided into individual populations based on seven equal regions (0.2 log units). The MFI values for ORAI1 and IFN-γ within each region were plotted. Results from two animals are shown. Data are representative of six experiments. $R^2$ represents the coefficient of determination.

The data from our studies suggest a model whereby functional dysregulation in lung effector cells occurs at the level of the CRAC channel. This interpretation is based on the following results: the reduction in ORAI1 mRNA and protein, the increased calcium flux observed following treatment with 2-APB, and the restoration of function in cells stimulated in the presence of high levels of extracellular calcium. Active regulation at the level of the CRAC channel is a previously unappreciated mechanism for the negative control of T cell effector function and contrasts with previous studies of nonfunctional T cells, wherein calcium defects have been attributed to dysregulation of TCR proximal events. In light of this model, it is of interest that T cells isolated from the intestinal lamina propria are hyporesponsive to TCR engagement [55, 56]. This decreased responsiveness is associated with a decreased calcium signal in these cells [55, 56]. It is tempting to speculate that these mucosal T cells may share a similar regulation at the level of the CRAC channel. However, this awaits further study.

The most straightforward model for the inability of the cells to function is that limiting the CRAC channel number results in insufficient calcium entry necessary for the production of cytokines or the release of lytic granules. The inability of T cells to function as a result of a defect in the CRAC channel function has been reported [57]. T cells from SCID patients express a mutant form of ORAI1, which results in a defect in SOCE and NFAT activation. In our nonfunctional cells, which exhibit decreased levels of ORAI1, one scenario is that reduced calcium uptake is the result of inefficient assembly of the CRAC channel. The functional CRAC channel requires dimerization of ORAI1 dimers that reside in the plasma membrane [33, 58]. An overall decrease in ORAI1 dimers may make assembly of the functional channel more difficult. STIM1 has been shown recently to be responsible for the re-

quired dimerization [33] and as such, plays a crucial role in CRAC channel regulation. However, although we found that the STIM1 message was lower in nonfunctional cells, the reduction was relatively modest. Nonetheless, it remains possible that STIM1 contributes to dysregulation of calcium uptake. The decrease in the ORAI1 message observed in nonfunctional cells was reflected in a reduction in ORAI1 protein, albeit to a lesser extent. In these analyses, we also observed a correlation within functional cells between the level of ORAI1 protein and the amount of IFN-γ produced, suggesting that regulation of CRAC channel expression may also contribute to the quality of effector cells. Whether such a correlation exists in lymph node effector cells is unknown. If so, it would suggest the level of ORAI1 may determine/predict the amount of cytokine produced by a cell. If this correlation is restricted to lung effectors, the reduction in ORAI1 may instead mark cells that are in the early stages of functional impairment.

In light of our findings, it is interesting that T cells in the lung have been reported to exhibit higher baseline levels of cytoplasmic calcium compared with cells in the spleen [59]. Given previous findings that calcium signaling in the absence of AP-1 and NF-κB activation results in the induction of an anergy program of gene expression [38], it is tempting to speculate that signals in the lung result in a sustained, low-level calcium signal in effector cells. This partial signal resulting in the activation of NFAT1 in the absence of AP-1 and NF-κB may promote expression of one or more genes involved in the negative regulation of CRAC channel expression.

The question remains as to why effector cells present in the lung should exhibit such a profound loss-of-function. We would propose that this is an attempt by the host to limit damage to this fragile, critical tissue. Evidence to support this model comes from studies of influenza infection [60]. In those analyses, effector cells present in the lung were found to be disabled through engagement of NKG2A. When mice lacking the NKG2A ligand Qa-1b were infected, loss-of-function in effectors was prevented. Not surprisingly, this resulted in increased immunopathology in the lung. Thus, the number of effectors dictates the extent to which pathology is associated with viral clearance. This suggests that turning off effector cell function is a strategy used by the host to limit destruction of the vitally important lung tissue.

In conclusion, our findings show that loss-of-function in lung effector cells is associated with a reduction in CRAC channel expression, which leads to decreased calcium flux and NFAT1 activation. Loss-of-function as a result of CRAC channel regulation is a novel mechanism for functional dysregulation of effector cells in the periphery. Future studies to further dissect the control of ORAI1 expression in these cells may open the door to the development of new therapeutics that have the capability to inhibit or enhance function of effector T cells as desired.

## AUTHORSHIP

Subhashini Arimilli: execution and analysis of most experiments and manuscript preparation; Sharad K. Sharma: Western blot analyses; Rama Yammani: assistance in execution of functional assays; Sean D. Reid: real-time PCR analyses; Griffith D. Parks: growth and characterization of virus; Martha A. Alexander-Miller: experimental design, interpretation, and manuscript preparation.

## ACKNOWLEDGMENTS

This work was supported by grant R01 HL071985 (to M. A. A-M.). We acknowledge the National Institutes of Health Tetramer Facility for provision of tetramer. We are grateful to Dr. Jason Grayson for helpful discussions regarding the manuscript.

### REFERENCES

1. Chang, J., Braciale, T. J. (2002) Respiratory syncytial virus infection suppresses lung $CD8^+$ T-cell effector activity and peripheral $CD8^+$ T-cell memory in the respiratory tract. *Nat. Med.* **8,** 54–60.
2. Vallbracht, S., Unsold, H., Ehl, S. (2006) Functional impairment of cytotoxic T cells in the lung airways following respiratory virus infections. *Eur. J. Immunol.* **36,** 1434–1442.
3. Claassen, E. A., van der Kant, P. A., Rychnavska, Z. S., van Bleek, G. M., Easton, A. J., van der Most, R. G. (2005) Activation and inactivation of antiviral CD8 T cell responses during murine pneumovirus infection. *J. Immunol.* **175,** 6597–6604.
4. Fulton, R. B., Olson, M. R., Varga, S. M. (2008) Regulation of cytokine production by virus-specific CD8 T cells in the lungs. *J. Virol.* **82,** 7799–7811.
5. Gray, P. M., Arimilli, S., Palmer, E. M., Parks, G. D., Alexander-Miller, M. A. (2005) Altered function in CD8+ T cells following paramyxovirus infection of the respiratory tract. *J. Virol.* **79,** 3339–3349.
6. Zajac, A. J., Blattman, J. N., Murali-Krishna, K., Sourdive, D. J., Suresh, M., Altman, J. D., Ahmed, R. (1998) Viral immune evasion due to persistence of activated T cells without effector function. *J. Exp. Med.* **188,** 2205–2213.
7. Shin, H., Wherry, E. J. (2007) CD8 T cell dysfunction during chronic viral infection. *Curr. Opin. Immunol.* **19,** 408–415.
8. Gruener, N. H., Lechner, F., Jung, M. C., Diepolder, H., Gerlach, T., Lauer, G., Walker, B., Sullivan, J., Phillips, R., Pape, G. R., Klenerman, P. (2001) Sustained dysfunction of antiviral CD8+ T lymphocytes after infection with hepatitis C virus. *J. Virol.* **75,** 5550–5558.
9. Schwartz, R. H. (2003) T cell anergy. *Annu. Rev. Immunol.* **21,** 305–334.
10. Rodriguez, P. C., Ochoa, A. C. (2006) T cell dysfunction in cancer: role of myeloid cells and tumor cells regulating amino acid availability and oxidative stress. *Semin. Cancer Biol.* **16,** 66–72.
11. Demotte, N., Stroobant, V., Courtoy, P. J., Van Der, S. P., Colau, D., Luescher, I. F., Hivroz, C., Nicaise, J., Squifflet, J. L., Mourad, M., Godelaine, D., Boon, T., van der Bruggen, P. (2008) Restoring the association of the T cell receptor with CD8 reverses anergy in human tumor-infiltrating lymphocytes. *Immunity* **28,** 414–424.
12. Nagaraj, S., Gupta, K., Pisarev, V., Kinarsky, L., Sherman, S., Kang, L., Herber, D. L., Schneck, J., Gabrilovich, D. I. (2007) Altered recognition of antigen is a mechanism of CD8+ T cell tolerance in cancer. *Nat. Med.* **13,** 828–835.
13. Bandyopadhyay, S., Soto-Nieves, N., Macian, F. (2007) Transcriptional regulation of T cell tolerance. *Semin. Immunol.* **19,** 180–187.
14. Zhong, X. P., Guo, R., Zhou, H., Liu, C., Wan, C. K. (2008) Diacylglycerol kinases in immune cell function and self-tolerance. *Immunol. Rev.* **224,** 249–264.
15. Saibil, S. D., Deenick, E. K., Ohashi, P. S. (2007) The sound of silence: modulating anergy in T lymphocytes. *Curr. Opin. Immunol.* **19,** 658–664.
16. Arimilli, S., Palmer, E. M., Alexander-Miller, M. A. (2008) Loss of function in virus-specific lung effector T cells is independent of infection. *J. Leukoc. Biol.* **83,** 564–574.
17. Oh-hora, M., Rao, A. (2008) Calcium signaling in lymphocytes. *Curr. Opin. Immunol.* **20,** 250–258.
18. Feske, S. (2007) Calcium signaling in lymphocyte activation and disease. *Nat. Rev. Immunol.* **7,** 690–702.
19. Borde, M., Barrington, R. A., Heissmeyer, V., Carroll, M. C., Rao, A. (2006) Transcriptional basis of lymphocyte tolerance. *Immunol. Rev.* **210,** 105–119.
20. Zheng, Y., Zha, Y., Gajewski, T. F. (2008) Molecular regulation of T-cell anergy. *EMBO Rep.* **9,** 50–55.
21. Wu, M. M., Buchanan, J., Luik, R. M., Lewis, R. S. (2006) $Ca2^+$ store depletion causes STIM1 to accumulate in ER regions closely associated with the plasma membrane. *J. Cell Biol.* **174,** 803–813.
22. Luik, R. M., Wu, M. M., Buchanan, J., Lewis, R. S. (2006) The elementary unit of store-operated Ca2+ entry: local activation of CRAC channels by STIM1 at ER-plasma membrane junctions. *J. Cell Biol.* **174,** 815–825.

23. Sica, A., Dorman, L., Viggiano, V., Cippitelli, M., Ghosh, P., Rice, N., Young, H. A. (1997) Interaction of NF-κB and NFAT with the interferon-γ promoter. *J. Biol. Chem.* **272,** 30412–30420.
24. Sweetser, M. T., Hoey, T., Sun, Y. L., Weaver, W. M., Price, G. A., Wilson, C. B. (1998) The roles of nuclear factor of activated T cells and ying-yang 1 in activation-induced expression of the interferon-γ promoter in T cells. *J. Biol. Chem.* **273,** 34775–34783.
25. Wansley, E. K., Dillon, P. J., Gainey, M. D., Tam, J., Cramer, S. D., Parks, G. D. (2005) Growth sensitivity of a recombinant simian virus 5 P/V mutant to type I interferon differs between tumor cell lines and normal primary cells. *Virology* **335,** 131–144.
26. Gray, P. M., Parks, G. D., Alexander-Miller, M. A. (2001) A novel CD8-independent high-avidity cytotoxic T-lymphocyte response directed against an epitope in the phosphoprotein of the paramyxovirus simian virus 5. *J. Virol.* **75,** 10065–10072.
27. Reid, S. D., Green, N. M., Sylva, G. L., Voyich, J. M., Stenseth, E. T., DeLeo, F. R., Palzkill, T., Low, D. E., Hill, H. R., Musser, J. M. (2002) Postgenomic analysis of four novel antigens of group A streptococcus: growth phase-dependent gene transcription and human serologic response. *J. Bacteriol.* **184,** 6316–6324.
28. Bas, A., Forsberg, G., Hammarstrom, S., Hammarstrom, M. L. (2004) Utility of the housekeeping genes 18S rRNA, β-actin and glyceraldehyde-3-phosphate-dehydrogenase for normalization in real-time quantitative reverse transcriptase-polymerase chain reaction analysis of gene expression in human T lymphocytes. *Scand. J. Immunol.* **59,** 566–573.
29. Rao, A. (2009) Signaling to gene expression: calcium, calcineurin and NFAT. *Nat. Immunol.* **10,** 3–5.
30. Vig, M., Kinet, J. P. (2009) Calcium signaling in immune cells. *Nat. Immunol.* **10,** 21–27.
31. Luik, R. M., Lewis, R. S. (2007) New insights into the molecular mechanisms of store-operated Ca2+ signaling in T cells. *Trends Mol. Med.* **13,** 103–107.
32. Prakriya, M., Lewis, R. S. (2001) Potentiation and inhibition of $Ca^{2+}$ release-activated $Ca^{2+}$ channels by 2-aminoethyldiphenyl borate (2-APB) occurs independently of IP(3) receptors. *J. Physiol.* **536,** 3–19.
33. Penna, A., Demuro, A., Yeromin, A. V., Zhang, S. L., Safrina, O., Parker, I., Cahalan, M. D. (2008) The CRAC channel consists of a tetramer formed by Stim-induced dimerization of ORAI dimers. *Nature* **456,** 116–120.
34. Almeida, J. R., Price, D. A., Papagno, L., Arkoub, Z. A., Sauce, D., Bornstein, E., Asher, T. E., Samri, A., Schnuriger, A., Theodorou, I., Costagliola, D., Rouzioux, C., Agut, H., Marcelin, A. G., Douek, D., Autran, B., Appay, V. (2007) Superior control of HIV-1 replication by CD8+ T cells is reflected by their avidity, polyfunctionality, and clonal turnover. *J. Exp. Med.* **204,** 2473–2485.
35. Precopio, M. L., Betts, M. R., Parrino, J., Price, D. A., Gostick, E., Ambrozak, D. R., Asher, T. E., Douek, D. C., Harari, A., Pantaleo, G., Bailer, R., Graham, B. S., Roederer, M., Koup, R. A. (2007) Immunization with vaccinia virus induces polyfunctional and phenotypically distinctive CD8(+) T cell responses. *J. Exp. Med.* **204,** 1405–1416.
36. Betts, M. R., Nason, M. C., West, S. M., De Rosa, S. C., Migueles, S. A., Abraham, J., Lederman, M. M., Benito, J. M., Goepfert, P. A., Connors, M., Roederer, M., Koup, R. A. (2006) HIV nonprogressors preferentially maintain highly functional HIV-specific CD8+ T cells. *Blood* **107,** 4781–4789.
37. Monu, N., Frey, A. B. (2007) Suppression of proximal T cell receptor signaling and lytic function in CD8+ tumor-infiltrating T cells. *Cancer Res.* **67,** 11447–11454.
38. Macian, F., Garcia-Cozar, F., Im, S. H., Horton, H. F., Byrne, M. C., Rao, A. (2002) Transcriptional mechanisms underlying lymphocyte tolerance. *Cell* **109,** 719–731.
39. Heissmeyer, V., Macian, F., Im, S. H., Varma, R., Feske, S., Venuprasad, K., Gu, H., Liu, Y. C., Dustin, M. L., Rao, A. (2004) Calcineurin imposes T cell unresponsiveness through targeted proteolysis of signaling proteins. *Nat. Immunol.* **5,** 255–265.
40. Lupher Jr., M. L., Songyang, Z., Shoelson, S. E., Cantley, L. C., Band, H. (1997) The Cbl phosphotyrosine-binding domain selects a D(N/D)XpY motif and binds to the Tyr292 negative regulatory phosphorylation site of ZAP-70. *J. Biol. Chem.* **272,** 33140–33144.
41. Barber, D. L., Wherry, E. J., Masopust, D., Zhu, B., Allison, J. P., Sharpe, A. H., Freeman, G. J., Ahmed, R. (2006) Restoring function in exhausted CD8 T cells during chronic viral infection. *Nature* **439,** 682–687.
42. Jurado, J. O., Alvarez, I. B., Pasquinelli, V., Martinez, G. J., Quiroga, M. F., Abbate, E., Musella, R. M., Chuluyan, H. E., Garcia, V. E. (2008) Programmed death (PD)-1:PD-ligand 1/PD-ligand 2 pathway inhibits T cell effector functions during human tuberculosis. *J. Immunol.* **181,** 116–125.
43. Chemnitz, J. M., Parry, R. V., Nichols, K. E., June, C. H., Riley, J. L. (2004) SHP-1 and SHP-2 associate with immunoreceptor tyrosine-based switch motif of programmed death 1 upon primary human T cell stimulation, but only receptor ligation prevents T cell activation. *J. Immunol.* **173,** 945–954.
44. Parry, R. V., Chemnitz, J. M., Frauwirth, K. A., Lanfranco, A. R., Braunstein, I., Kobayashi, S. V., Linsley, P. S., Thompson, C. B., Riley, J. L. (2005) CTLA-4 and PD-1 receptors inhibit T-cell activation by distinct mechanisms. *Mol. Cell. Biol.* **25,** 9543–9553.
45. Acuto, O., Di Bartolo, V., Michel, F. (2008) Tailoring T-cell receptor signals by proximal negative feedback mechanisms. *Nat. Rev. Immunol.* **8,** 699–712.
46. Dubois, P. M., Pihlgren, M., Tomkowiak, M., Van Mechelen, M., Marvel, J. (1998) Tolerant CD8 T cells induced by multiple injections of peptide antigen show impaired TCR signaling and altered proliferative responses in vitro and in vivo. *J. Immunol.* **161,** 5260–5267.
47. Kimura, M., Yamashita, M., Kubo, M., Iwashima, M., Shimizu, C., Tokoyoda, K., Chiba, J., Taniguchi, M., Katsumata, M., Nakayama, T. (2000) Impaired Ca/calcineurin pathway in in vivo anergized CD4 T cells. *Int. Immunol.* **12,** 817–824.
48. Diehl, S., Chow, C. W., Weiss, L., Palmetshofer, A., Twardzik, T., Rounds, L., Serfling, E., Davis, R. J., Anguita, J., Rincon, M. (2002) Induction of NFATc2 expression by interleukin 6 promotes T helper type 2 differentiation. *J. Exp. Med.* **196,** 39–49.
49. Wu, W., Misra, R. S., Russell, J. Q., Flavell, R. A., Rincon, M., Budd, R. C. (2006) Proteolytic regulation of nuclear factor of activated T (NFAT) c2 cells and NFAT activity by caspase-3. *J. Biol. Chem.* **281,** 10682–10690.
50. Weitzel, R. P., Lesniewski, M. L., Haviernik, P., Kadereit, S., Leahy, P., Greco, N. J., Laughlin, M. J. (2009) microRNA 184 regulates expression of NFAT1 in umbilical cord blood CD4+ T cells. *Blood* **113,** 6648–6657.
51. Yoeli-Lerner, M., Yiu, G. K., Rabinovitz, I., Erhardt, P., Jauliac, S., Toker, A. (2005) Akt blocks breast cancer cell motility and invasion through the transcription factor NFAT. *Mol. Cell* **20,** 539–550.
52. Liou, J., Kim, M. L., Heo, W. D., Jones, J. T., Myers, J. W., Ferrell Jr., J. E., Meyer, T. (2005) STIM is a Ca2+ sensor essential for Ca2+-store-depletion-triggered Ca2+ influx. *Curr. Biol.* **15,** 1235–1241.
53. Mercer, J. C., Dehaven, W. I., Smyth, J. T., Wedel, B., Boyles, R. R., Bird, G. S., Putney Jr., J. W. (2006) Large store-operated calcium selective currents due to co-expression of ORAI1 or ORAI2 with the intracellular calcium sensor, STIM1. *J. Biol. Chem.* **281,** 24979–24990.
54. Zhang, S. L., Yu, Y., Roos, J., Kozak, J. A., Deerinck, T. J., Ellisman, M. H., Stauderman, K. A., Cahalan, M. D. (2005) STIM1 is a Ca2+ sensor that activates CRAC channels and migrates from the Ca2+ store to the plasma membrane. *Nature* **437,** 902–905.
55. Schwarz, A., Tutsch, E., Ludwig, B., Schwarz, E. C., Stallmach, A., Hoth, M. (2004) Ca2+ signaling in identified T-lymphocytes from human intestinal mucosa. Relation to hyporeactivity, proliferation, and inflammatory bowel disease. *J. Biol. Chem.* **279,** 5641–5647.
56. Tutsch, E., Griesemer, D., Schwarz, A., Stallmach, A., Hoth, M. (2004) Two-photon analysis of calcium signals in T lymphocytes of intact *Lamina propria* from human intestine. *Eur. J. Immunol.* **34,** 3477–3484.
57. Feske, S., Gwack, Y., Prakriya, M., Srikanth, S., Puppel, S. H., Tanasa, B., Hogan, P. G., Lewis, R. S., Daly, M., Rao, A. (2006) A mutation in ORAI1 causes immune deficiency by abrogating CRAC channel function. *Nature* **441,** 179–185.
58. Vig, M., Beck, A., Billingsley, J. M., Lis, A., Parvez, S., Peinelt, C., Koomoa, D. L., Soboloff, J., Gill, D. L., Fleig, A., Kinet, J. P., Penner, R. (2006) CRACM1 multimers form the ion-selective pore of the CRAC channel. *Curr. Biol.* **16,** 2073–2079.
59. Strickland, D., Kees, U. R., Holt, P. G. (1996) Regulation of T-cell activation in the lung: isolated lung T cells exhibit surface phenotypic characteristics of recent activation including down-modulated T-cell receptors, but are locked into the G0/G1 phase of the cell cycle. *Immunology* **87,** 242–249.
60. Zhou, J., Matsuoka, M., Cantor, H., Homer, R., Enelow, R. I. (2008) Cutting edge: engagement of NKG2A on $CD8^+$ effector T cells limits immunopathology in influenza pneumonia. *J. Immunol.* **180,** 25–29.


KEY WORDS:
$CD8^+$ T cell · function · regulation · NFAT · TCR signal transduction